C. R. Chimie 16 (2013) 937–944

Contents lists available at SciVerse ScienceDirect

Comptes Rendus Chimie

www.sciencedirect.com

Full paper/Mémoire

Intermolecular spin–spin coupling constants between ^{31}P atoms

Dionisia Sanz [a], Rosa M. Claramunt [a], François Mathey [b], Ibon Alkorta [c,*], Goar Sánchez-Sanz [c], José Elguero [c]

[a] Departamento de Química Orgánica y Bio-Orgánica, Facultad de Ciencias, Universidad Nacional de Educación a Distancia (UNED), Senda del Rey 9, 28040 Madrid, Spain
[b] Division of Chemistry and Biological Chemistry, School of Physical and Mathematical Sciences, Nanyang Technological University, 50, Nanyang Avenue, Singapore 639798, Singapore
[c] Instituto de Química Médica, Centro de Química Orgánica "Manuel Lora-Tamayo", CSIC, Juan de la Cierva, 3, 28006 Madrid, Spain

ARTICLE INFO

Article history:
Received 15 March 2013
Accepted after revision 28 May 2013
Available online 30 July 2013

Keywords:
Pnictogen bonds
CPMAS NMR
Intermolecular ^{31}P–^{31}P couplings
DFT calculations

Mots clés:
Liaisons pnictogènes
RMN CPMAS
Couplages intermoléculaires ^{31}P–^{31}P
Calculs DFT

ABSTRACT

This paper reports the study by NMR spectroscopy and ab initio methods of the structure of 3,4-dimethyl-1-cyanophosphole and its dimer. The dimer presents a P···P interaction of the pnictogen type due to the presence of σ-holes. NMR of the monomer was recorded in $CDCl_3$ solution while NMR of the dimer corresponds to the solid state (CPMAS) experiments. The $^{2p}J_{PP}$ spin–spin coupling constant has not been measured, but calculated at the B3LYP level. AIM, NBO and ELF methodologies have been used to describe the electronic structure of the dimer.

RÉSUMÉ

Cette communication décrit l'étude par RMN et par des calculs ab initio de la structure du diméthyl-3,4-cyano-1-phosphole et de son dimère. Le dimère présente une interaction P···P du type pnictogène due à la présence d'un trou σ. Le spectre RMN du monomère a été enregistré dans le $CDCl_3$ tandis que celui du dimère provient de spectres CPMAS (état solide). Il n'a pas été possible de mesurer le couplage $^{2p}J_{PP}$, mais sa valeur a été calculée aux niveaux B3LYP et MP2. Les méthodes AIM, NBO et ELF ont été utilisées pour décrire la structure électronique du dimère.

1. Introduction

The interest in weak interactions and their properties increases continuously. Amongst the most recent and less known are the pnictogen bonds [1–3]. There are several methods to characterize these bonds: geometries (obtained by crystallography and other techniques), calculated interaction energies, electron densities, IR and UV bands, NMR chemical shifts, etc. [1] NMR spin–spin coupling constants (SSCC) provide important information about their electronic structure. Experimentally, such SSCC termed $^{1p}J_{PP}$ in the case of both pnictogen atoms being phosphorus, have been observed in intramolecular situations with the unavoidable problem of the transmission of the spin information through the skeleton linking both ^{31}P atoms [1]. A large variety of intermolecular pnictogen complexes [2–7] and one intramolecular case [8] have been calculated theoretically. Closely related to this topic is the σ-hole concept [9].

Although the interaction energies for dimer stabilization are quite large (up to 35 kJ mol^{-1} for PH_2F dimer) [4], there is small hope to measure $^{1p}J_{PP}$ in solution. In 1988, one of us described 3,4-dimethyl-1-cyanophosphole (**1**) and described many of its NMR properties (Table 1) [10]. In

* Corresponding author.
E-mail address: ibon@iqm.csic.es (I. Alkorta).

1631-0748/$ – see front matter © 2013 Académie des sciences. Published by Elsevier Masson SAS. All rights reserved.
http://dx.doi.org/10.1016/j.crci.2013.05.016

Table 1
Experimental chemical shifts in $CDCl_3$ (ppm) and SSCC (absolute values, Hz) for monomer 1.

Atom	Group	Experimental [10]	Experimental (this work)
^{1}H	CH_3	2.13, $^{4}J_{HH} = \|0.7\|$, $^{4}J_{HP} = \|3.6\|$	
	2,5 (CH)	6.27, $^{4}J_{HH} = \|0.7\|$, $^{2}J_{HP} = \|42.0\|$	
^{13}C	CH_3	17.3, $^{3}J_{CP} = \|3.6\|$	17.8, $^{1}J_{CH} = 127.8$, $^{3}J_{CH} \sim 4.6$, $^{3}J_{CP} = \|5.0\|$
	CN	115.9, $^{1}J_{CP} = \|83.0\|$	116.1, $^{3}J_{CH} = {}^{5}J_{CH} \sim 3$, $^{1}J_{CP} = \|82.9\|$
	2,5 (CH)	120.5, singlet[a]	120.4, $^{1}J_{CH} = 176.5$, $^{3}J_{CH} = 6.0$ (Me), $^{3}J_{CH} = 3.6$
	3,4	155.5, $^{2}J_{CP} = \|8.5\|$	155.6, $^{2}J_{CP} = \|8.8\|$
^{15}N	CN	[b]	
^{31}P (**1**)	Ring	−54.7	−52.5, $^{1}J_{CP} = \|83.0\|$[c]

[a] That means that $^{1}J_{CP} \leq |2|$ Hz.
[b] This signal is not observed even after long time.
[c] Measured on the ^{13}C satellites.

2001, the X-ray structure of **1** was reported (Fig. 1) [11]. It is a dimer ($\mathbf{1}_2$) with a P···P distance of 3.384 Å. In the CSD, the compound received the EDIJOQ refcode [12].

2. Experimental

2.1. Chemistry

The synthesis of compound **1** was reported in references [10] and [11].

2.2. NMR

Solution NMR spectra were recorded on a Bruker DRX 400 (9.4 Tesla, 400.13 MHz for ^{1}H, 100.62 MHz for ^{13}C, 161.96 for ^{31}P) spectrometer with a 5-mm inverse-detection H–X probe equipped with a *z*-gradient coil, at 300 K. Chemical shifts (δ in ppm) are given from internal solvent, $CDCl_3$ 7.26 for ^{1}H and 77.0 for ^{13}C; for ^{31}P NMR 85% H_3PO_4 (0.0) was used as the external standard. Coupling constants (J in Hz) are accurate to ± 0.2 Hz for ^{1}H and ± 0.6 Hz for ^{13}C and ^{31}P, respectively.

Solid state ^{13}C (100.73 MHz), ^{31}P (162.16 MHz) and ^{15}N (40.60 MHz) CPMAS NMR spectra have been obtained on a Bruker WB 400 spectrometer at 300 K using a 4 mm DVT probehead. Samples were carefully packed in a 4-mm diameter cylindrical zirconia rotor with Kel-F end-caps. Operating conditions involved 3.2 μs 90° ^{1}H pulses and decoupling field strength of 78.1 kHz by TPPM sequence. ^{13}C spectra were originally referenced to a glycine sample and then, the chemical shifts were recalculated to the Me_4Si [for the carbonyl atom δ (glycine) = 176.1 ppm], ^{31}P spectra to $(NH_4)_2HPO_4$ (AHP) and ^{15}N spectra to $^{15}NH_4Cl$ and then converted to nitromethane scale using the relationship: δ $^{15}N(MeNO_2) = \delta$ $^{15}N(NH_4Cl) - 338.1$ ppm. Typical acquisition parameters for ^{13}C CPMAS were: spectral width, 40 kHz; recycle delay, 5 s; acquisition time, 30 ms; contact time, 2 ms; and spin rate, 12 kHz. In order to distinguish between protonated and unprotonated carbon atoms, the NQS (non-quaternary suppression) experiment by conventional cross-polarization was recorded; before the acquisition, the decoupler is switched off for a very short time of 25 μs [13,14]. Typical acquisition parameters for ^{31}P CPMAS were: spectral width, 100 kHz; recycle delay, 5 s; acquisition time, 30 ms; contact time, 2 ms; and spin rate, 10 and 12 kHz. Typical acquisition parameters for ^{15}N CPMAS were: spectral width, 40 kHz; recycle delay, 5 s; acquisition time, 35 ms; contact time, 6 ms; and spin rate, 6 kHz.

2.3. Computational details

The geometry of the systems has been optimized at the MP2 computational level [15] with the aug′-cc-pVTZ basis set [16]. This basis set is derived from the Dunning aug-cc-pVTZ basis set by removing diffuse functions from H atoms. The absolute chemical shielding and coupling constants of the systems have been calculated with the GIAO method [17] at the B3LYP/aug′-cc-pVTZ level [18].

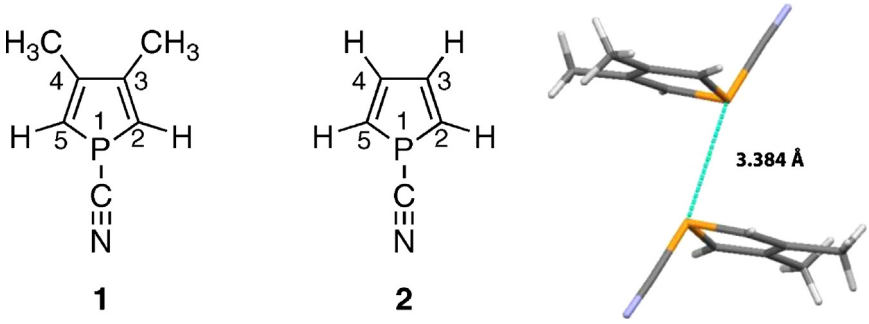

Fig. 1. Monomer **1**, model compound **2** and structure of the dimer EDIJOQ ($\mathbf{1}_2$). Color available online.

The Gaussian-09 program has been used for these calculations [19].

The electronic properties of the system have been analyzed through molecular electrostatic potential (MEP), electron density [20], electron localization function (ELF) [21] and natural bond orbitals (NBO) [22] measurements. The MEP has been calculated with the Gaussian-09 program and has been represented on the 0.001 au electron density isosurface with the WFA program [23]. This program has been used to analyze the local minima and maxima of the MEP on the surface. The topological analysis of the electron density has been carried out with the AIMAll program [24]. The topological analysis of the electron density provides the critical points of this property. AIM permits to define the molecular graph of the investigated systems as the ensemble of maxima of the electron density, ρ, associated with the position of the nuclei, saddle points, in which ρ, has two negative and one positive curvatures, the so-called bond critical points (BCPs) and the zero gradient lines connecting them, or bond paths. The ELF function allows to detect those region where the electrons are more concentrated. Thus, information of the characteristics of the different types of bond and lone pair are easily obtained. The ELF function has been calculated with the Topmod program [25]. The natural bond orbital (NBO) method has been used to obtain atomic charges and to analyze the orbital charge transfer between the interactions molecules. The NBO-3 program has been used for these calculations [26].

3. Results and discussion

3.1. NMR spectroscopy

In NMR, using $CDCl_3$ as solvent, monomer **1** is characterized by the data reported in Table 1.

Our attempts to add more data to Table 1 mostly failed: the ^{15}N chemical shifts cannot be measured probably because the signal is a doublet ($^2J_{PN}$) without near H atoms. Moreover, $^2J_{PN}$ cannot be measured on the ^{15}N satellites of the ^{31}P signal because the coupling is buried inside the central peak. In our hands, the ^{31}P NMR signal appears at –52.5 ppm instead of –54.7 ppm [10] (a concentration effect, calculated for the monomer –61.7 and for the dimer –60.3 ppm) and its ^{13}C satellites corresponds to a $^1J_{CP} = |83.0|$ (Fig. 2). An isotope effect of 0.05 ppm (8.1 Hz) between ^{31}P–^{12}C and ^{31}P–^{13}C is also observed in Fig. 2. The $^2J_{NP}$ coupling constant of 18.9 Hz (calculated, Table 2) is lost under the central peak. Since the ^1H decoupling was not complete, the lateral peaks due to $^2J_{HP} = 42.0$ Hz coupling were observed, where these peaks are split by the $^4J_{HP} = 3.6$ Hz (in principle, a septuplet, but only the three central lines were observed).

Then, we calculated theoretically the chemical shifts and coupling constants of **1** (Table 2). The calculations correspond to geometries optimized at the MP2/aug′-cc-pVTZ. On these optimized geometries, we carried out GIAO and SSCC calculations at the B3LYP/aug′-cc-pVTZ level [for references, see Section 2.3].

The calculations afford absolute shieldings (σ, ppm). To transform them into chemical shifts, we have used

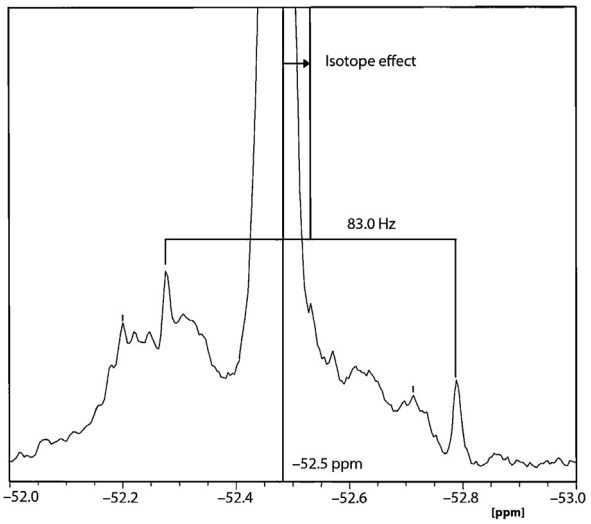

Fig. 2. ^{31}P [^1H] NMR spectrum of **1** in $CDCl_3$ at 161.96 MHz.

Table 2
Calculated absolute shieldings (ppm) for compound **1** and SSCC (Hz) for compounds **1** and **2**.

Atom	Group	δ **1**	SSCC **1**	SSCC **2**
^1H	CH_3	2.36	$^4J_{HH} = -1.3$, $^4J_{HP} = +4.8$	–
	2,5 (CH)	6.61	$^4J_{HH} = -1.3$, $^2J_{HP} = +45.0$	–
^{13}C	CH_3	17.8	$^3J_{CP} = +3.4$	–
	CN	114.5	$^1J_{CP} = -97.2$	$^1J_{CP} = -86.4$
	2,5 (CH)	126.4	$^1J_{CP} = -8.4$	$^1J_{CP} = -10.3$
	3,4	156.3	$^2J_{CP} = +10.1$	$^2J_{CP} = +12.1$
^{15}N	CN	–82.2	$^1J_{CN} = -7.6$	$^1J_{CN} = -8.0$
^{31}P (**1**)	Ring	–61.7	$^2J_{NP} = +18.9$	$^2J_{NP} = +19.0$

empirical equations established with many compounds of the largest diversity for GIAO/B3LYP/6-311++G(d,p) calculations. It is important to note that solvent effects are included in these equations since they have been obtained by comparing calculated values in the gas phase with experimental values in solution. Using data of nitriles and isonitriles [27], we have calculated the equation for the ^{15}N chemical shifts of these compounds.

$$\delta^1H = 31.0 - 0.97 * \sigma^1H \text{ (reference TMS, 0.00 ppm) [28]}$$

$$\delta^{13}C = 175.7 - 0.963 * \sigma^{13}C \text{ (reference TMS, 0.00 ppm) [29]}$$

$$\delta^{15}N = -153.4 - 0.744 * \sigma^{15}N$$
$$\text{(referenceext., neat } MeNO_2\text{, 0.00 ppm) [thiswork]}$$

$$\delta^{31}P = 237.0 - 0.81 * \sigma^{31}P$$
$$\text{(referenceext., 85\% } H_3PO_4 \text{ ppm) [30]}$$

These equations are probably different for B3LYP/aug′-cc-pVTZ calculations but allow us to compare different calculations and, for some nuclei, are rather good. For instance, the experimental chemical shifts of compound **1** in $CDCl_3$ (Table 1) are well correlated with the calculated values of Table 2.

$$\delta_{exp} = (1.7 \pm 1.5) + (0.970 \pm 0.016)\,\delta_{calc}, n = 7, R^2 = 0.999$$

Comparing the values for **1** and **2**, we note that the methyl groups at positions 3 and 4 exert a small influence

Table 3
Experimental and calculated [with the minimum (3.21 Å) and the X-ray (3.38 Å) P···P distances] chemical shifts (ppm) for dimer $\mathbf{1}_2$.

Atom	Group	Experimental (CPMAS)	Calculated minimum	Calculated X-ray
^{13}C	CH_3	18.4 (s)	17.7	17.7
	CN	118.25 (m)	114.8	114.7
	2,5 (CH)	120.25 (s)	128.0	126.3
	3,4	158.8 (s[a])	157.1	156.5
^{15}N	CN	−80.1 (s[b])	−80.1	−78.4
^{31}P (**1**)	Ring	−55.6 (s[c])	−62.3	−60.3

[a] C3/C4 (158.8, NQS) is a singlet. This is consistent with $^2J_{CP}$ = 11.4.
[b] The full width at half maximum (WHM) is about 0.5 ppm, that is, 20 Hz.
[c] The full width at half maximum (WHM) is about 0.86 ppm, that is, 140 Hz, see Fig. 5.

Table 4
Calculated (gas phase) SSCC (Hz) for dimers $\mathbf{1}_2$ and $\mathbf{2}_2$, with the minimum (3.21 Å) and the X-ray (3.38 Å) P···P distances.

Atom	Group	SSCC $\mathbf{1}_2$ minimum	SSCC $\mathbf{1}_2$ X-ray	SSCC $\mathbf{2}_2$ X-ray
^1H	CH_3	$^4J_{HH}$ = −1.5, $^4J_{HP}$ = +4.4	$^4J_{HH}$ = −1.5, $^4J_{HP}$ = +4.9	–
	2,5 (CH)	$^4J_{HH}$ = −1.5, $^2J_{HP}$ = +42.2	$^4J_{HH}$ = −1.5, $^2J_{HP}$ = +42.8	–
^{13}C	CH_3	$^3J_{CP}$ = +4.4	$^3J_{CP}$ = +4.6	–
^{13}C	CN	$^1J_{CP}$ = −96.0	$^1J_{CP}$ = −94.4	$^1J_{CP}$ = −84.6
	2,5 (CH)	$^1J_{CP}$ = −4.0, $^{2p}J_{CP}$ = +0.6	$^1J_{CP}$ = −3.8, $^{2p}J_{CP}$ = +0.3	$^1J_{CP}$ = −5.9, $^{2p}J_{CP}$ = −0.1
	3,4	$^2J_{CP}$ = +9.1	$^2J_{CP}$ = +11.5	$^2J_{CP}$ = +11.4
^{15}N	CN	$^1J_{CN}$ = −8.2, $^2J_{NP}$ = +19.1 $^{2p}J_{CP}$ = +17.5	$^1J_{CN}$ = −8.3, $^2J_{NP}$ = +19.2 $^{2p}J_{CP}$ = +9.7	$^1J_{CN}$ = −8.7, $^2J_{NP}$ = +19.0 $^{2p}J_{CP}$ = +12.3
^{31}P (**1**)	Ring	$^{1p}J_{PP}$ = +163.2	$^{1p}J_{PP}$ = +101.8	$^{1p}J_{PP}$ = +133.4

on the coupling constants, the most affected being $^1J_{CP}$ (difference 10.8 Hz).

Both the chemical shifts and SSCC of **1** are acceptably calculated, the worse result concerns $^1J_{CP}$ is calculated to be −97.2 (experimental 83.0 Hz) and −8.4 Hz (experimental $< |2|$ Hz). Thus, we have calculated the SSCC of the dimer (Table 3) to see if the value of $^{1p}J_{PP}$ was experimentally attainable.

Using all the available data from the monomer and the dimer, the following equations are obtained:

$\delta_{exp} = (1.6 \pm 1.2) + (0.977 \pm 0.012)\ \delta_{calc\ (minimum)}$, $n = 13$, $R^2 = 0.998$, predicted, ^{15}N (Table 1) −78.7

$\delta_{exp} = (1.1 \pm 1.2) + (0.984 \pm 0.012)\ \delta_{calc\ (X\text{-}ray)}$, $n = 13$, $R^2 = 0.998$, predicted ^{15}N (Table 1) −79.7

Both equations are very similar even for the predictions for the missing value of the monomer in Table 1.

Concerning dimer $\mathbf{1}_2$, if we compare the calculations based on the minimum and on the X-ray geometry, only $^{2p}J_{CP}$ (1.8 factor) and $^{1p}J_{PP}$ (1.6 factor) are affected. Comparing **1** with $\mathbf{1}_2$ and **2** with $\mathbf{2}_2$ (X-ray P···P distance), the most affected SSCC is $^1J_{CP}$ of the CH that decrease to a half (from about −9 to about −4 Hz). The most important result of Table 4 is the sensitivity of the couplings through the pnictogen bond: $^{2p}J_{CP}$ from +17.5 to +9.7 Hz and $^{1p}J_{PP}$ from +163.2 to +101.8 Hz.

The ^{13}C experimental results are shown in Fig. 3 (normal) and Fig. 4 (NQS), while the ^{31}P CPMAS spectrum is depicted in Fig. 5.

For determining the $^{1p}J_{PP}$ in the solid state of the dimer of 3,4-dimethyl-1-cyanophosphole (**1**), two situations are possible:

- the symmetry is lifted in the solid state, in spite of the high symmetry obtained by X-ray crystallography (C_{2h}). In this case, the ^{31}P CPMAS spectrum contains two signals. If $J_{P\cdots P}$ is larger than the line width, then one could see an AX or AB spin system and hence, $J_{P\cdots P}$. That being the easiest case;
- the symmetry is not lifted in the solid state.

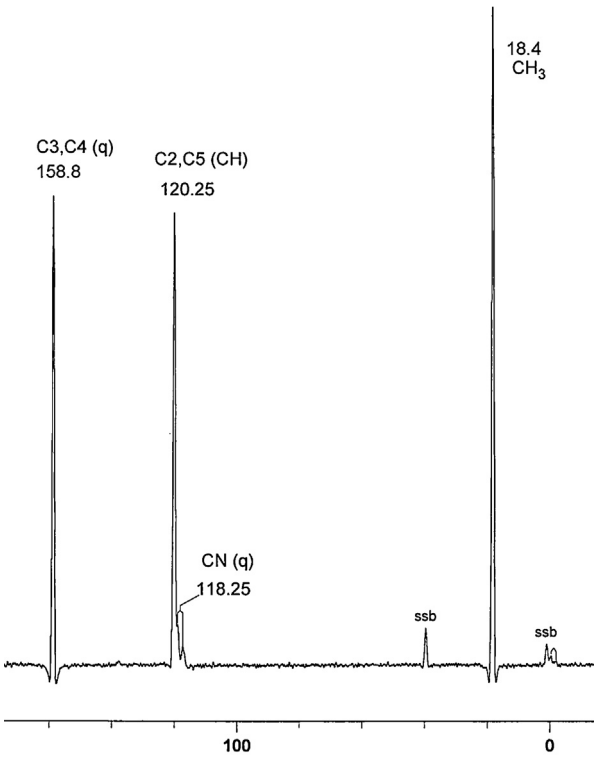

Fig. 3. $^{13}C/^1H$ CPMAS NMR spectrum of $\mathbf{1}_2$.

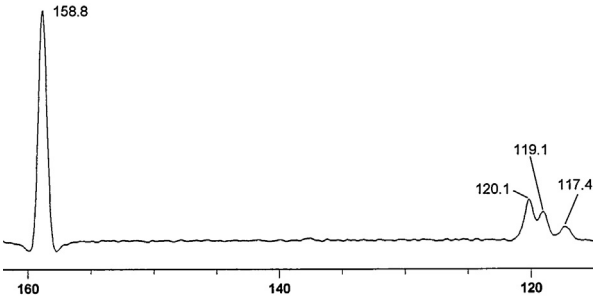

Fig. 4. NQS. The 120.1 ppm signal is a residual of the CH. The signals at 118.25 (119.1 and 117.4 ppm) belong to the CN.

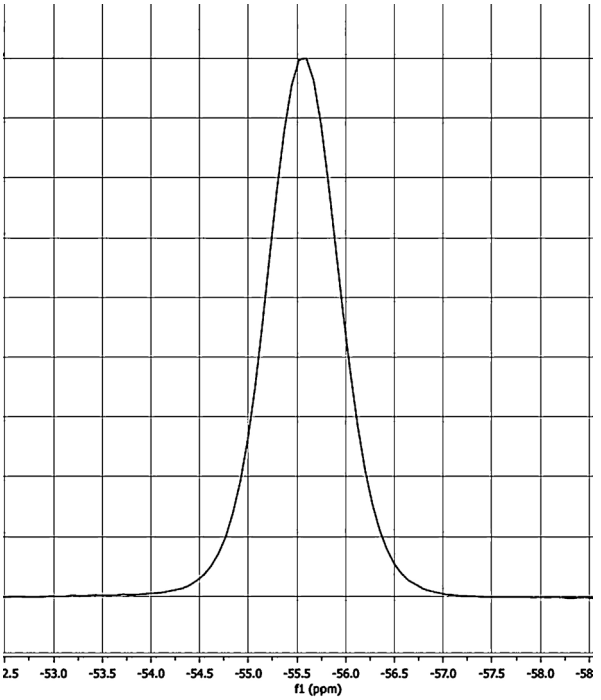

Fig. 5. ^{31}P CPMAS spectrum of $\mathbf{1}_2$.

Methods used to measure $J_{P\cdots P}$:

- the ^{31}P spectrum shows only a single signal (Fig. 5). Under MAS conditions, it is difficult to measure $J_{P\cdots P}$. However, by single crystal ^{31}P NMR it would be possible [31] because due to the chemical shift anisotropy, the two ^{31}P will not be chemically equivalent for many different orientations. Unfortunately, single crystals of **1** of suitable size for NMR studies [31] cannot be prepared;
- another possibility is to try the use of the ^{13}C satellites in ^{31}P NMR. ^{31}P near ^{12}C and ^{13}C have different chemical shifts, but the difference might be small;
- a better approach would be to analyze the ^{13}C signal of the cyano group, and proceed in a similar way as some of us do previously, using ^{15}N labeled samples [32].

We tried the second method but as it can be seen in Fig. 5, no ^{13}C satellites were observed. Taking into account that the full width at half maximum (WHM) is about 140 Hz and that the calculated values for $^{1p}J_{PP}$ are ~102 Hz (X-ray geometry) and ~163 Hz (minimum geometry), it is not surprising that this approach failed. Then, we tried the third method. In Fig. 4, three signals were observed near 120 ppm: 120.1 ppm corresponds to a residual of the C2, C5 CHs (120.25 ppm in Fig. 3) and 119.1 and 117.4 ppm corresponding to the CN (118.25 ppm in Fig. 3, note that they are apparent in the spinning-side band near 0 ppm). The signal at 119.1 ppm is more intense than that at 117.4 ppm, but this may be due to overlapping with the 120.1 ppm signal; these signals are separated by 169.5 Hz. This cannot be due to the $^{1}J_{CP}$ because for the monomer its values are 83.0 (experimental, Table 1) and −97.2 Hz (calculated, Table 2) and for the dimer they are −96.0 (calculated, Table 4, minimum geometry) and −94.4 Hz (calculated, Table 4, X-ray geometry). Therefore, this "apparent" doublet is the X part of an AA′X system (A ^{31}P–^{12}C, A′ ^{31}P–^{13}C and X ^{13}C). The difference between A and A′ can be estimated to be $\Delta\nu \sim 8$ Hz (from the monomer), $J_{A'X} = -80/-85$ Hz, $J_{AX} = 10/20$ Hz and $J_{AA'} = 100/160$ Hz. But lacking the small transitions of the X part of an AA′X system, it was not possible to carry out an analysis of the spin system to ascertain the values of these couplings.

3.2. Theoretical results

3.2.1. Monomers

It has been shown in the literature that in most weak interactions complexes, the electrostatic term is the most important one [33]. In the case of the pnictogen interactions, the presence of an electronegative group bonded to the P atom generates a region of positive charge, named in the literature as σ-hole [34]. This σ-hole interacts with an electron-rich region, such as a lone pair. In the case of symmetrical P···P interactions, two simultaneous σ-hole:-lone pair interactions can be found.

In the systems studied in this paper, the cyano group generates a σ-hole with a value of 0.017 and 0.022 au, for **1** and **2**, respectively (Fig. 6).

3.2.2. Dimers

Two minima, A and B, have been found in the optimization of $\mathbf{1}_2$ and $\mathbf{2}_2$ dimers in gas phase. In the case of **1**, the most stable one B corresponds to two P···π pnictogen bond ($E_i = -46.4$ kJ mol^{-1}). This value of Ei is considerably higher that the stronger Ei reported in the introduction (−35 kJ mol^{-1}). The disposition of the monomers within the dimers studied could favor some extra stabilization similar to the π–π stacking found between aromatic rings.

The second minima ($E_i = -37.1$ kJ mol^{-1}) is analogous to the one found in the crystal structure and present a P···P pnictogen bond. In the case of **2**, the relative stability of the two dimers is reversed and the one with a P···P interaction shows a stabilization energy of −29.8 kJ mol^{-1} while the one with P···π contacts corresponds to −27.2 kJ mol^{-1}.

The intermolecular P···P distances in $\mathbf{1}_2$ and $\mathbf{2}_2$ are 3.21 and 3.19 Å, which is approximately 0.2 Å shorter than the

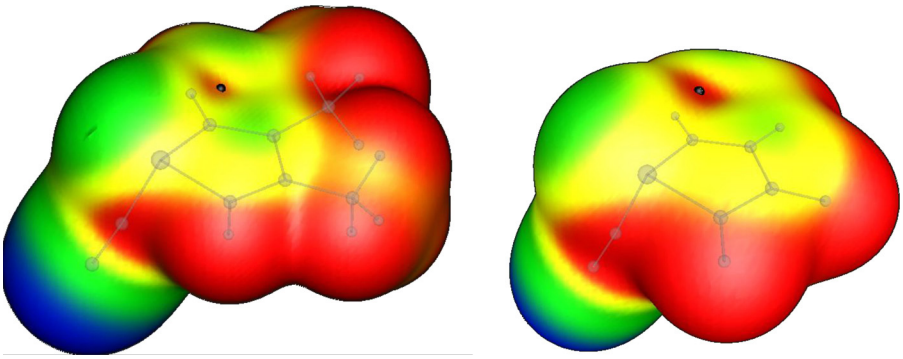

Fig. 6. MEP on the 0.001 au electron density isosurface. Left **1**, right **2**. The black dot indicates the position of the σ-hole. Color code for the MEP (au): red > 0.015 > yellow > 0.0 > green > –0.03 > blue.

distance found in the solid phase. Fixing the intermolecular distance to that in the solid phase, the interaction energies of the dimers obtained are only 1.4 and 1.1 kJ mol^{-1} less stable, respectively, than the dimers without restrictions.

The topological analysis of the electron density (Fig. 7) shows a P···P bond for the dimers analogous to the one found in the solid phase and two P···π for the alternative dimer and interactions between the heterocyclic rings. In

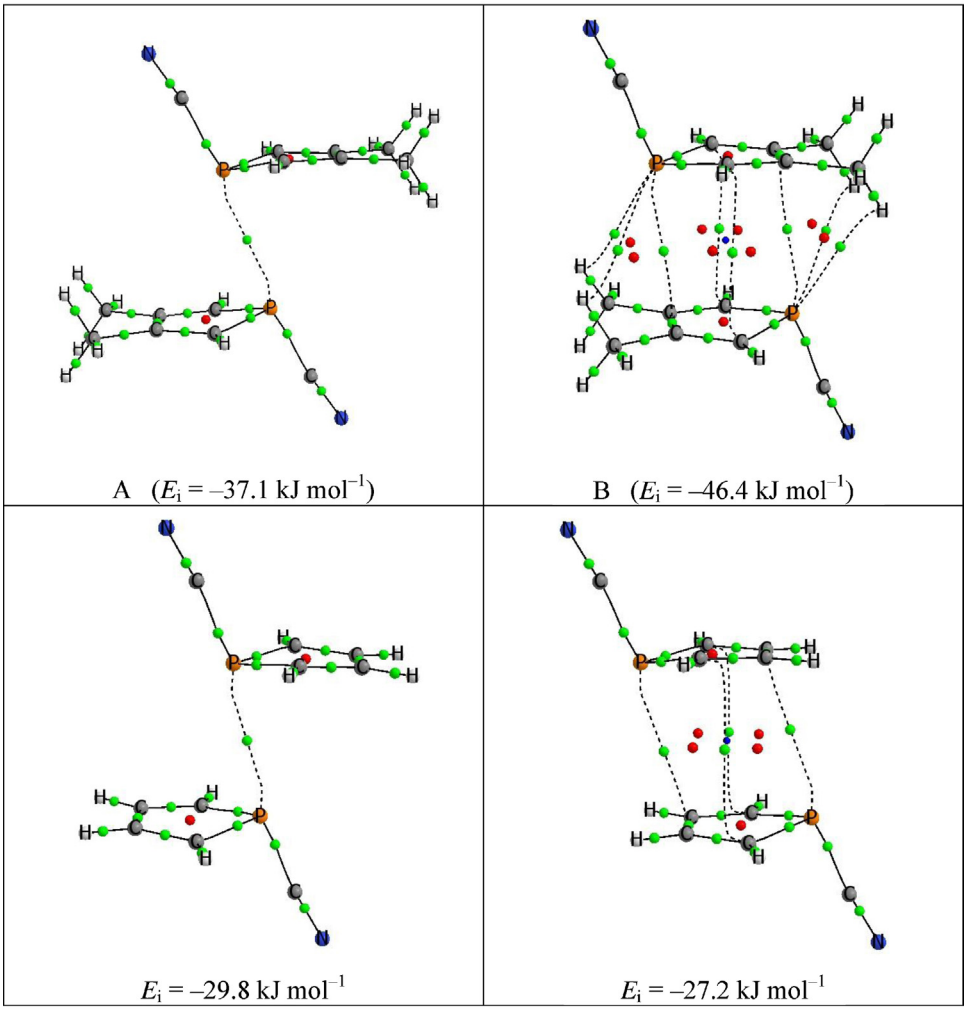

Fig. 7. Molecular graphs of the dimers studied. Green, red and blue dots indicate the position of the bond, ring and cage critical points, respectively. The lines connecting the atoms correspond to the bond path.

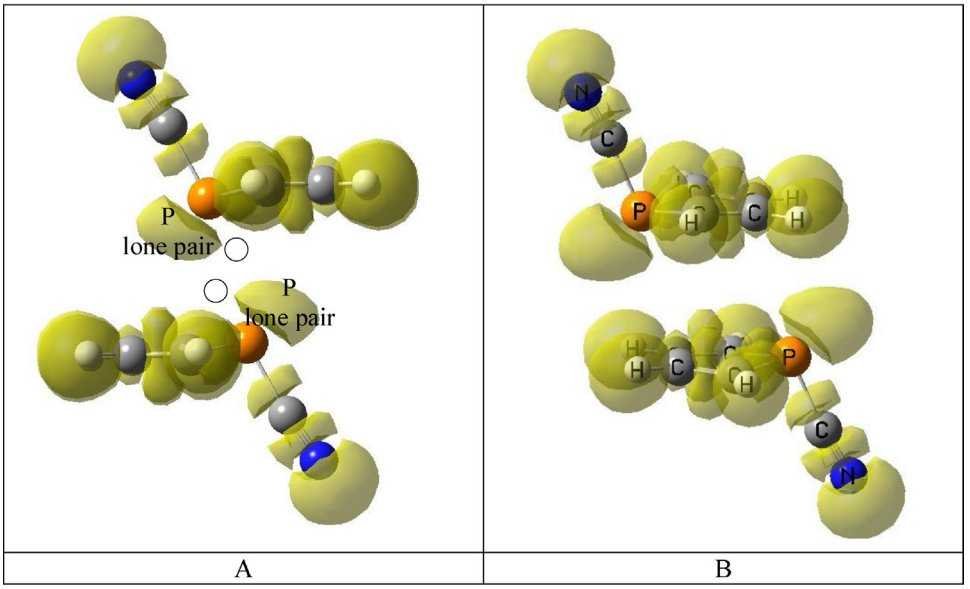

Fig. 8. ELF 0.75 isosurface. The P lone pair basins are indicated. The empty circle indicates the approximate position of the σ-hole. Color available on line.

the case of $\mathbf{1}_2$, some additional interactions between the methyl groups and the P atoms are also found.

The NBO analysis shows two degenerate orbital interactions between the lone pair of the P atom of one molecule and the σ^* P-C of the other one in the A dimers (12.0 and 14.1 kJ mol^{-1} for $\mathbf{1}_2$ and $\mathbf{2}_2$, respectively) while in the B dimers, the charge transfer between intermolecular orbitals are very small (less than 2.5 kJ mol^{-1}).

The representation of the ELF (Fig. 8) shows that the lone pair of the P atoms of one molecule is located in the extension of the NC-P bond of the other molecule, where the σ-hole generated by the NC-P bond should be located.

For the B dimers, the σ-hole points toward the centre of the C3–C4 bond of the phosphole.

4. Conclusions

Although the experimental values of the intermolecular coupling constant between two ^{31}P atoms have not been determined, the study of the dimer of 3,4-dimethyl-1-cyanophosphole (1) has provided interesting information about this complex. The use of NMR, both in solution (monomer) and in the solid state (dimer), coupled with ab initio calculations, has confirmed that $^{2p}J_{PP}$ coupling constants are large enough to be measured in other complexes. The topological analysis of the electron density and the electron localization function representation illustrates the pnictogen interactions as well as the position of the σ-hole.

Acknowledgments

We thank Prof Hans-Heinrich Limbach and Drs María Luisa Jimeno and Alain Fruchier for valuable discussions on the experimental determination of SSCC in the solid state. Thanks are also given to the Ministerio de Ciencia e Innovación of Spain (Projects CTQ2012-13129-C02-02 and CTQ2010-16122) and the Comunidad Autónoma de Madrid (Project MADRISOLAR2, ref. S2009/PPQ-1533).

References

[1] S. Bauer, S. Tschirschwitz, P. Înnecke, R. Frank, B. Kirchner, L. Matthew, L.M. Clarke, E. Hey-Hawkins, Eur. J. Inorg. Chem. (2009) 2776.
[2] S. Zahn, R. Frank, E. Hey-Hawkins, B. Kirchner, Chem. Eur. J. 17 (2011) 6034.
[3] S. Scheiner, J. Chem. Phys. 134 (2011) 094315.
[4] J.E. Del Bene, I. Alkorta, G. Sánchez-Sanz, J. Elguero, Chem. Phys. Lett. 512 (2011) 184.
[5] J.E. Del Bene, I. Alkorta, G. Sánchez-Sanz, J. Elguero, J. Phys. Chem. A 116 (2012) 3056.
[6] J.E. Del Bene, G. Sánchez-Sanz, I. Alkorta, J. Elguero, Chem. Phys. Lett. 538 (2012) 14.
[7] I. Alkorta, G. Sánchez-Sanz, J. Elguero, J.E. Del Bene, J. Chem. Theor. Comput. 8 (2012) 2320.
[8] G. Sánchez-Sanz, I. Alkorta, C. Trujillo, J. Elguero, J.E. Del Bene, Chem. Phys. Chem. (2013), cphc.201300145, in press.
[9] (a) P. Politzer, K.E. Riley, F.A. Bulat, J.S. Murray, Comput. Theoret. Chem. 998 (2012) 2 ;
(b) P. Politzer, J.S. Murray, Chem. Phys. Chem. 14 (2013) 278.
[10] S. Holand, F. Mathey, Orgametallics 7 (1988) 1796.
[11] E. Mattmann, D. Simonutti, L. Ricard, F. Mercier, F. Mathey, J. Org. Chem. 66 (2001) 755.
[12] (a) F.H. Allen, Acta Crystallogr. Sect. B 58 (2002) 380 ;
(b) F.H. Allen, W.D.S. Motherwell, Acta Crystallogr. Sect. B 58 (2002) 407 ;
(c) CSD version 5.32, updated Feb. 2011. http://www.ccdc.cam.ac.uk.
[13] P.D. Murphy, J. Magn. Reson. 52 (1983) 343, ibid. 62 (1985) 303.
[14] L.B. Alemany, D.M. Grant, T.D. Alger, R.J. Pugmire, J. Am. Chem. Soc. 105 (1982) 6697.
[15] C. Møller, M.S. Plesset, Phys. Rev. 46 (1934) 618.
[16] (a) T.H. Dunning, J. Chem. Phys. 90 (1989) 1007 ;
(b) D.E. Woon, T.H. Dunning, J. Chem. Phys. 103 (1995) 4572.
[17] (a) R. Ditchfield, Mol. Phys. 27 (1974) 789 ;
(b) F. London, J. Phys. Radium 8 (1937) 397.
[18] (a) A.D. Becke, J. Chem. Phys. 98 (1993) 5648 ;
(b) C.S. Lee, W. Yang, R.G. Parr, Phys. Rev. B 37 (1988) 785.
[19] M.J. Frisch, G.W. Trucks, H.B. Schlegel, G.E. Scuseria, M.A. Robb, J.R. Cheeseman, G. Scalmani, V. Barone, B. Mennucci, G.A. Petersson, H. Nakatsuji, M. Caricato, X. Li, H.P. Hratchian, A.F. Izmaylov, J. Bloino, G.

Zheng, J.L. Sonnenberg, M. Hada, M. Ehara, K. Toyota, R. Fukuda, J. Hasegawa, M. Ishida, T. Nakajima, Y. Honda, O. Kitao, H. Nakai, T. Vreven, J.A. Montgomery Jr., J.E. Peralta, F. Ogliaro, M. Bearpark, J.J. Heyd, E. Brothers, K.N. Kudin, V.N. Staroverov, R. Kobayashi, J. Normand, K. Raghavachari, A. Rendell, J.C. Burant, S.S. Iyengar, J. Tomasi, M. Cossi, N. Rega, J.M. Millam, M. Klene, J.E. Knox, J.B. Cross, V. Bakken, C. Adamo, J. Jaramillo, R. Gomperts, R.E. Stratmann, O. Yazyev, A.J. Austin, R. Cammi, C. Pomelli, J.W. Ochterski, R.L. Martin, K. Morokuma, V.G. Zakrzewski, G.A. Voth, P. Salvador, J.J. Dannenberg, S. Dapprich, A.D. Daniels, Ö. Farkas, J.B. Foresman, J.V. Ortiz, J. Cioslowski, D.J. Fox, Gaussian 09. Revision A. 1, Gaussian, Inc, Wallingford CT, USA, 2009.

[20] (a) R.F.W. Bader, Atoms in molecules: a quantum theory, in : J. Halpen, M.L.H. Green (Eds.), The International Series of Monographs of Chemistry, Clarendon Press, Oxford, 1990 ;
(b) P.L.A. Popelier, Atoms in Molecules: An Introduction, Prentice Hall, London, 2000.

[21] B. Silvi, A. Savin, Nature 371 (1994) 683.

[22] A.E. Reed, L.A. Curtiss, F. Weinhold, Chem. Rev. 88 (1988) 899.

[23] F. Bulat, A. Toro-Labbé, T. Brinck, J. Murray, P. Politzer, J. Mol. Model. 16 (2010) 1679.

[24] T.A. Keith, T.K. Aimall, Gristmill Software (aim.tkgristmill.com), Overland Park KS, USA, 2012.

[25] A. Savin, B. Silvi, F. Coionna, Can. J. Chem. 74 (1996) 1088.

[26] E.D. Glendening, A.E. Reed, J.E. Carpenter, F. Weinhold, NBO 3.1 Program.

[27] (a) S. Berger, S. Braun, H.O. Kalinowski, NMR Spectroscopy of the Non-Metallic Elements, John Wiley & Sons, Chichester, 1997p. 153 ;
(b) S.J. Goede, F.J.J. de Kanter, F. Bickelhaupt, J. Am. Chem. Soc. 113 (1991) 6104.

[28] A.M.S. Silva, R.M.S. Sousa, M.L. Jimeno, F. Blanco, I. Alkorta, J. Elguero, Magn. Reson. Chem. 46 (2008) 859.

[29] F. Blanco, I. Alkorta, J. Elguero, Magn. Reson. Chem. 45 (2007) 797.

[30] I. Alkorta, F. Blanco, J. Elguero, J. Mol. Struct. (Theochem) 942 (2010) 1.

[31] (a) M.D. Lumsden, K. Eichele, R.E. Wasylishen, T.S. Cameron, J.F. Britten, J. Am. Chem. Soc. 116 (1994) 11129 ;
(b) K. Eichele, R.E. Wasylishen, J. Phys. Chem. 98 (1994) 3108 ;
(c) M.J. Potrzebowski, G. Grossmann, K. Ganicz, S. Olejniczak, W. Ciesielski, A.E. Koziol, I. Wawrzycka, G. Bujacz, U. Haeberlen, H. Schmitt, Chem. Eur. J. 8 (2002) 2691 ;
(d) G. Buntkowsky, H.H. Limbach, J. Low Temp. Phys. 143 (2006) 55.

[32] M. Pietrzak, J. Wehling, H.H. Limbach, N.S. Golubev, C. López, R.M. Claramunt, J. Elguero, J. Am. Chem. Soc. 123 (2001) 4338.

[33] (a) S. Karthikeyan, R. Sedlak, P. Hobza, J. Phys. Chem. A 115 (2011) 9422 ;
(b) G. Sánchez-Sanz, C. Trujillo, I. Alkorta, J. Elguero, Phys. Chem. Chem. Phys. 14 (2012) 9880 ;
(c) S.N. Steinmann, C. Piemontesi, A. Delachat, C. Corminboeuf, J. Chem. Theor. Comput. 8 (2012) 1629.

[34] P. Politzer, P. Lane, M. Concha, Y. Ma, J. Murray, J. Mol. Model. 13 (2007) 305.